Assessing muscle co-activation dynamics by counting motor evoked potentials

Aslan Bellmann

01.04.2022

Abstract. Human motor control arguably relies on the propagation of neural commands to groups of muscles, called synergies. In non-human primates, considerable evidence for muscle synergies stems from neural stimulation research. Meanwhile, in humans, evidence is still scarce. Here, we applied transcranial magnetic stimulation to twenty subjects, recording electrophysiological responses from eight muscles acting on the fingers and the wrist. We hypothesized that muscles that are frequently used together might be grouped into synergies and thus have a higher tendency for co-activation. Previous studies used the Jaccard index to quantify co-activation in this context. We argue that the Jaccard index is not suitable for this context as it is biased by the excitability of individual muscles, and that pointwise mutual information should be used instead. Applying both measures to our data, we find a greater Jaccard index between thumb and index finger muscles and between wrist flexors, whose grouped activation is expected in everyday life during precision grip and wrist flexion, respectively. However, greater pointwise mutual information was only evident between wrist flexors. Therefore, it appears that the frequent co-activation of thumb and index finger muscles might be due to their high response probabilities, rather than due to synergistic coupling. We critically reflect on our findings, and discuss implications for future research on synergies in humans.

1 Introduction

Motor control has long been proposed to rely on synergies—groups of muscles that are activated as a single unit by the nervous system (Bernstein, 1966; Sherrington, 1952). Yet proper evidence remains limited. A common approach to studying synergies is to apply matrix factorization methods to voluntary electromyography (EMG) data. Rather than describing the EMG in terms of temporal activations of individual muscles, one considers it in terms of temporal activation of modules, which are composed of muscles with fixed weights ("spatial synergies") (Bach et al., 2021; Dominici et al., 2011; Ivanenko et al., 2004; Oliveira et al., 2016; Santuz et al., 2020) or fixed temporal activation patterns ("spatiotemporal synergies") (d'Avella et al., 2006; Overduin et al., 2008).

Modularity of voluntary EMG alone does not prove the existence of muscle synergies. Modularity may simply arise from biomechanical and task constraints (Kutch & Valero-Cuevas, 2012). Even if motor control relies on synergies, matrix factorization methods may not accurately identify them in the presence of such constraints (Steele et al., 2015). To circumvent these limitations, other approaches are needed (Cheung & Seki, 2021). Neural stimulation is one such alternative. Synergies that are hardwired into the nervous system should be detectable in kinematic and electrophysiological outputs evoked by the stimulation of the corresponding neural pathways.

In non-human primates, kinematic and electrophysiological responses to microstimulation present considerable evidence for muscle synergies. On the kinematic level, such stimulation has been shown to elicit ethologically meaningful compound movements (Graziano, 2016). On the electrophysiological level, such stimulation evokes EMG outputs which resemble voluntary EMG (Overduin et al., 2012; cf. Amundsen Huffmaster et al., 2017), and similar modules tend to be encoded at the same cortical site during stimulation and voluntary movement (Overduin et al., 2014). These studies provide evidence that synergies are activated by the cortex, but notably the synergies themselves may reside anywhere downstream along the motor pathway. Both corticospinal neurons (Shinoda et al., 1981) and spinal interneurons (Takei & Seki, 2010) are known to have divergent projections onto motoneurons. Spinal premotor interneurons have been shown to facilitate the activation of modules extracted from voluntary EMG during precision grip (Takei et al., 2017). One may hence argue that, in non-human primates, there is substantial evidence that motor control involves synergies. They can be activated cortically but seemingly reside, at least in part, in the spinal cord.

In humans, ethical constraints limit the invasiveness and thus the precision of cortical stimulation. Nevertheless, the kinematic responses to cortical stimulation lend some support for muscle synergies in humans. Stimulation via cortical surface electrodes has been shown to elicit ethologically meaningful movements in a subset of patients undergoing surgery (Desmurget et al., 2014). This seems to parallel the observations made in non-human primates. Notably, such movements could not be broken into individual components by reducing the stimulation intensity. In healthy humans, lack of direct, invasive access to the brain necessitates stimulation from outside the scalp, such as via transcranial magnetic stimulation (TMS) (Nollet et al., 2003). TMS over the cortical hand representation elicits multi-digit movements. The co-activation between individual digit kinematics is higher when evoked via TMS compared to when digits are moved passively (Gentner & Classen, 2006). This suggests that digits are coupled not only through mere biomechanics but also via neural factors. Here we would like to note, however, that this observation might be due to an artefact by means of stimulus spread, owing to the low spatial selectivity of TMS. That is, while stimulation-evoked kinematics appear compatible with the existence of muscle synergies in humans, that evidence should be considered weak.

There are also studies investigating the electrophysilogical responses to cortical stimulation in humans (DeJong et al., 2021; Melgari et al., 2008). These studies showed that TMS can elicit response in multiple muscles simultaneously. Furthermore, there was some evidence that muscles whose pairwise co-activation was more common amongst muscles that are commonly used together in everyday live, such as thumb and index finger muscles or different wrist extensors (DeJong et al., 2021). However, co-activation dynamics were quantified using the Jaccard index, which has important limitations (Salvatore et al., 2020). Thus, these studies should be interpreted with caution.

Following the same line, we applied TMS over the motor cortex and recorded electrophysiological responses from eight hand and forearm muscles. We compared co-activation dynamics between different hand and forearm muscle pairs. Regarding the quantification of co-activation dynamics, we argue that the Jaccard index is inappropriate in this context as it is confounded by the excitability of individual muscles. We argue, and demonstrate *in silico*, that pointwise mutual information is a better choice. For comparability, we apply both measures to our dataset. Here, we hypothesized that muscles which are naturally used together tend to be co-activated more often. In particular, we expected that thumb and index finger muscles tend to be co-activated more often than, for example, thumb and little finger muscles or index and little finger muscles. This is based on the simultaneous use of

the thumb and index finger in a highly delicate task: the precision grip (Maier & Hepp-Reymond, 1995). Furthermore, if moved with another digit, the thumb is most often moved with the index finger during natural digit use (Ingram et al., 2008).

2 Methods

We first present our argument, and outline the complementary *in silico* study, on how to quantify co-activation. Then, we describe the experimental study.

2.1 Theoretical Background and Simulation

Aiming to explore functional links between muscles, previous studies have delivered a series of TMS pulses and compared the pairwise co-activation of muscles within subjects (DeJong et al., 2021; Melgari et al., 2008). Co-activation was quantified using the Jaccard index: the number of occasions where both muscles were active normalized by the number of occasions where at least one of the two muscles was active. Here, we argue that the Jaccard index is a sub-optimal measure in this context and pointwise mutual information is a preferable alternative.

Consider a bivariate Bernoulli process $(X_1, Y_1), ..., (X_n, Y_n) \in \{0, 1\}^2$, where all the $\{X_i, Y_i\}$ are independent and identically distributed. Within the context of TMS, the $\{X_i, Y_i\}$ represent the on/off responses of two muscles to a series of n TMS pulses. With $i \in \mathbb{Z} : 1 \leq i \leq n$ and $x, y \in \{0, 1\}$, denote the individual unconditional probabilities

$$p_X(x) = P(\{X_i = x\}) \tag{1a}$$

$$p_Y(y) = P(\{Y_i = y\}), \tag{1b}$$

and the joint probability

$$p_{X,Y}(x, y) = P(\{X_i = x \cap Y_i = y\}). \tag{2}$$

The Jaccard index (Jaccard, 1912) then reads

$$\mathrm{JAC}(x, y) := \frac{p_{X,Y}(x, y)}{p_X(x) + p_Y(y) - p_{X,Y}(x, y)} = \left[\frac{p_X(x) + p_Y(y)}{p_{X,Y}(x, y)} - 1\right]^{-1}, \tag{3}$$

and the pointwise mutual information reads

$$\mathrm{PMI}(x, y) := \log \frac{p_{X,Y}(x, y)}{p_X(x) p_Y(y)}. \tag{4}$$

To highlight why we deem the Jaccard index inappropriate, let

$$\mathrm{R}(x,y) := \frac{p_{X,Y}(x,y)}{p_X(x)p_Y(y)}. \tag{5}$$

Of course, $\mathrm{R}(x,y)$ is the ratio of the expected co-occurrence of $\{X_i = x\}, \{Y_i = y\}$ to their expected co-occurrence if $\{X_i\}, \{Y_i\}$ were mutually independent. Thus, $\mathrm{R}(x,y)$ may be viewed as the 'degree of mutual dependence' between $\{X_i\}, \{Y_i\}$.

With this, the Jaccard index takes the form

$$\mathrm{JAC}(x,y) := \frac{\mathrm{R}(x,y)p_X(x)p_Y(y)}{p_X(x) + p_Y(y) - \mathrm{R}(x,y)p_X(x)p_Y(y)} = \left[\frac{p_X(x) + p_Y(y)}{\mathrm{R}(x,y)p_X(x)p_Y(y)} - 1\right]^{-1}. \tag{6}$$

The key issue is that the Jaccard index depends on all three parameters $\mathrm{R}(x,y), p_X(x), p_Y(y)$. Specifically, the partial derivatives are

$$\frac{\partial \mathrm{JAC}(x,y)}{\partial p_X(x)} = \frac{\mathrm{R}(x,y)p_Y^2(y)}{\left[\mathrm{R}(x,y)p_X(x)p_Y(y) - p_X(x) - p_Y(y)\right]^2} \tag{7a}$$

$$\frac{\partial \mathrm{JAC}(x,y)}{\partial p_Y(y)} = \frac{\mathrm{R}(x,y)p_X^2(x)}{\left[\mathrm{R}(x,y)p_X(x)p_Y(y) - p_X(x) - p_Y(y)\right]^2} \tag{7b}$$

$$\frac{\partial \mathrm{JAC}(x,y)}{\partial \mathrm{R}(x,y)} = \frac{p_X(x)p_Y(y)\left[p_X(x) + p_Y(y)\right]}{\left[\mathrm{R}(x,y)p_X(x)p_Y(y) - p_X(x) - p_Y(y)\right]^2}. \tag{8}$$

Equations (7a) and (7b) highlight a confounding effect: the Jaccard index increases with the individual probabilities. This confounding effect cannot be removed completely since it depends on $\mathrm{R}(x,y)$. [1] Equation (8) highlights the problem from a different angle: the effect of $\mathrm{R}(x,y)$ on the Jaccard index depends on the individual probabilities. Put differently, the Jaccard index poorly reflects the degree of mutual dependence. A more appropriate measure is the pointwise mutual information, which is fully determined by $\mathrm{R}(x,y)$,

$$\mathrm{PMI}(x,y) = \log \mathrm{R}(x,y). \tag{9}$$

[1] This confounding effect can only be removed for a specific $\mathrm{R}(x,y)$. Taking the difference of the Jaccard index from its hypothetical value at a specific $\mathrm{R}(x,y)$ removes the effect of the individual probabilities at that particular $\mathrm{R}(x,y)$. For example, Chung et al. (2019) used a 'centered Jaccard index', which is the difference of the Jaccard index from its hypothetical value under mutual independence. This removes the effect of the individual probabilities at $\mathrm{R}(x,y) = 1$ and allows to test whether $\mathrm{R}(x,y)$ is different from 1. However, the effect of the individual probabilities is still present at all $\mathrm{R}(x,y) \neq 1$. Thus, any comparison of the centered Jaccard index will be confounded by individual probabilities.

For illustration, we simulated $(X_1, Y_1), ..., (X_n, Y_n)$ using $p_X(x), p_Y(y) \in \{0.01, 0.02, ..., 0.99\}$ and $\mathrm{R}(x, y) \in \{1, 1.25, 1.5, 1.75\}$. We used $n = 500$ as this is similar to the number of stimulations delivered to each participant in our dataset. The probability axioms imply an additional constraint

$$\frac{p_X(x) + p_Y(y) - \min\left[p_X(x) + p_Y(y), 1\right]}{p_X(x)p_Y(y)} \leq \mathrm{R}(x, y) \leq \frac{1}{\max\left[p_X(x), p_Y(y)\right]}. \tag{10}$$

For each combination $\{p_X(x), p_Y(y), \mathrm{R}(x, y)\}$, we repeated the simulation $k = 100$ times and determined the average Jaccard index and the average pointwise mutual information across all repetitions, using empirical frequencies in place of probabilities.

2.2 Participants and Data Collection

The data we used was previously collected and used in a different study (Jin et al., 2021). Briefly, a series of TMS pulses was delivered to 20 healthy participants (eight females) with a mean age of 29.6 years (SD = 7.49 years). EMG was recorded from eight muscles—four hand muscles: adductor pollicis brevis (APB), flexor pollicis brevis (FPB), first dorsal interosseus (FDI), abductor digiti minimi (AMD), and four forearm muscles: flexor digitorum superficialis (FDS), extensor digitorum communis (EDC), flexor carpi radialis (FCR), extensor carpi radialis (ECR).

The coil position was pseudo-randomized, while the coil orientation was kept as constant as possible. The corresponding data was collected via a neuronavigation system. Each participant underwent two sessions, which were one hour apart. In each session, three stimulation intensities were used: 105% of the resting motor threshold (RMT) of FDI, FCR, and EDC. The low relative intensity of 105% RMT was chosen to limit stimulus spread (see Introduction). For subsequent data processing, data from both sessions and all stimulation intensities were pooled.

2.3 Data Processing

The eight muscles make 28 muscle pairs. For each muscle pair, we computed the Jaccard index and the pointwise mutual information, using empirical frequencies in place of probabilities. Pointwise mutual information was calculated using base-2 logarithms, and is thus given in bits.

2.4 Data Analysis

We analyzed both outcome measures using rank-based statistics. For pairs of hand muscles and pairs of forearm muscles, we used the Friedman test to test for main effects. If significant, we used the Nemenyi test to carry out pairwise comparisons. Since the Nemenyi test is designed to conserve the false positive error rate we did not apply any multiple comparisons adjustment. We set the false positive error rate to $\alpha = 0.05$.

2.5 Software and Code Availability

Data processing, analysis, and visualization was done in R (R Core Team, 2021), using the R packages 'colortools' (Sanchez, 2013), 'gdata' (Warnes et al., 2017), 'here' (Müller & Bryan, 2020), 'rcompanion' (Mangiafico, 2022), 'rstatix' (Kassambara, 2021), 'patchwork' (Pedersen, 2020), 'PMCMRplus' (Pohlert, 2021), and the collection of R packages 'tidyverse' (Wickham & RStudio, 2021). Data and code are available at https://github.com/motorlearner/project_tms_coactivation.

3 Results

3.1 Simulation

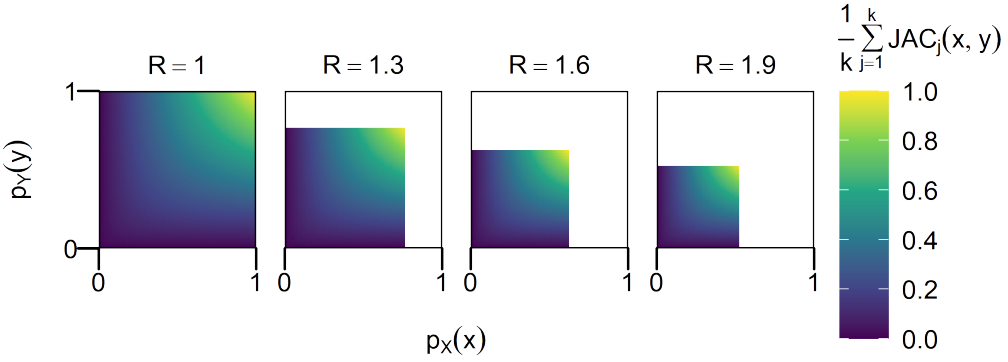

Figure 1: Mean Jaccard index (JAC) across $k = 100$ repetitions for different combinations of $p_X(x)$, $p_Y(y)$, and $\mathrm{R}(x, y)$. White areas are combinations that would violate the probability axioms.

Figure 1 shows the average Jaccard index and Figure 2 shows the average pointwise mutual

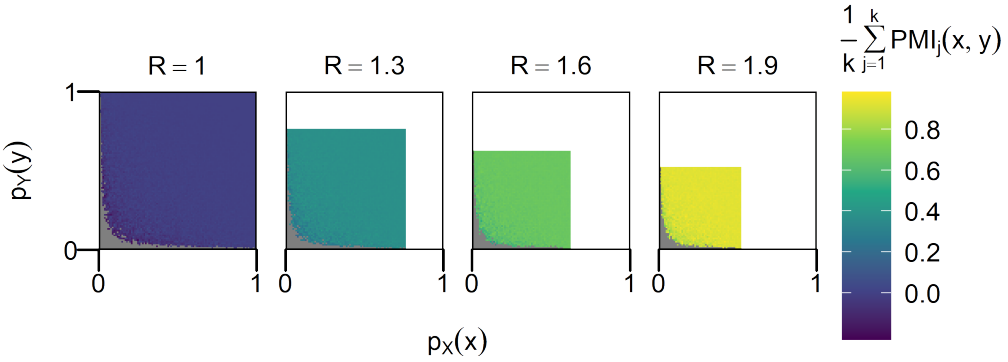

Figure 2: Mean pointwise mutual information (PMI) across $k = 100$ repetitions for different combinations of $p_X(x)$, $p_Y(y)$, and $\mathrm{R}(x, y)$. White areas are combinations that would violate the probability axioms. Gray areas denote values of $-\infty$.

information across all repetitions, for each combination $p_X(x)$, $p_Y(y)$, and $\mathrm{R}(x, y)$. The Jaccard index is not well suited to distinguish between different $\mathrm{R}(x, y)$, due to its dependency on $p_X(x)$ and $p_Y(y)$. In contrast, the pointwise mutual information scales directly with $\mathrm{R}(x, y)$.

Notably, with smaller $p_X(x)$ and $p_Y(y)$, the pointwise mutual information tended to be more variable and sometimes reached its theoretical minimum of $-\infty$. This highlights that $n = 500$ was not large enough to reliably estimate those probabilities. Generally, the joint probability is the smallest (since $p_{X,Y}(x, y) \leq \min\left[p_X(x), p_Y(y)\right]$). If the individual probabilities are small, the joint probability is usually even smaller and n needs to be large enough so that the expected number of joint occurrences between $\{X_i = x\}$ and $\{Y_i = y\}$ is sufficiently large. Pointwise mutual information estimates for small individual probabilities need to be interpreted in light of that limitation. This issue is further illustrated in Figure S1.

3.2 Collected Data

On average, a total of 639 (SD = 39.2) TMS pulses were delivered to each participant. The averages per stimulation protocol were 231 (SD = 26.1) when using the FDI RMT, 229 (SD = 18.7) when using the FCR RMT, and 233 (SD = 13.4) when using the EDC RMT. Figure 3 shows the Jaccard index and pointwise mutual information for all muscle pairs.

Figure 4 shows the Jaccard index and pointwise mutual information for hand muscle pairs

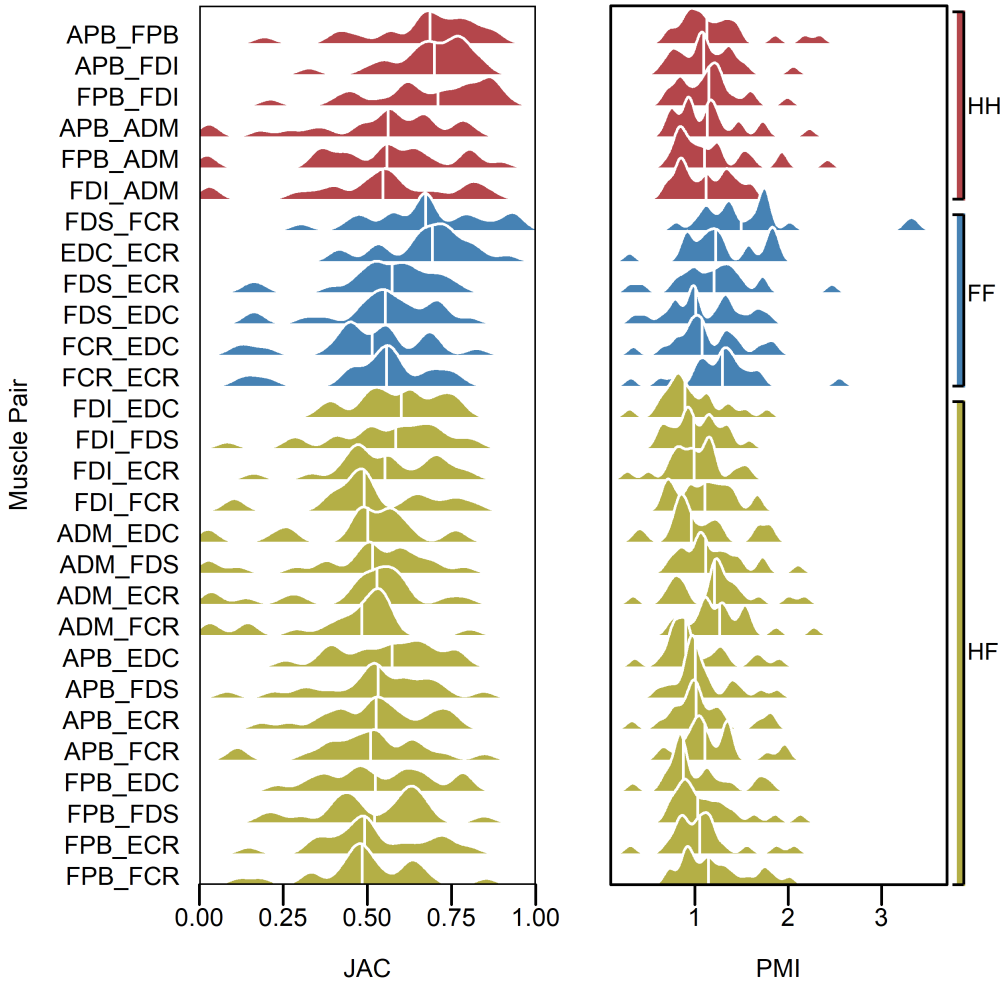

Figure 3: Jaccard index (JAC) and pointwise mutual information (PMI) for all muscle pairs. Densities were estimated using a Gaussian kernel with standard deviation ≈ 0.03 HH, *Hand-Hand*; FF, *Forearm-Forearm*; HF, *Hand-Forearm*.

only. There was a significant main effect for the Jaccard index ($p < 0.001$), and table S1 shows the p-values for subsequent pairwise comparisons. Thumb-index finger pairs had a significantly greater Jaccard index than most thumb-little finger pairs. Significantly greater Jaccard indices were also evident for one thumb-index finger pair compared to the index-little finger pairs, and for the thumb-thumb pair compared to one thumb-little finger pair. There was no significant main effect for the pointwise mutual information between hand muscle pairs ($p = 0.537$).

Figure 5 shows the Jaccard index and pointwise mutual information for forearm muscle pairs only. There was a significant main effect for the Jaccard index ($p < 0.001$), and

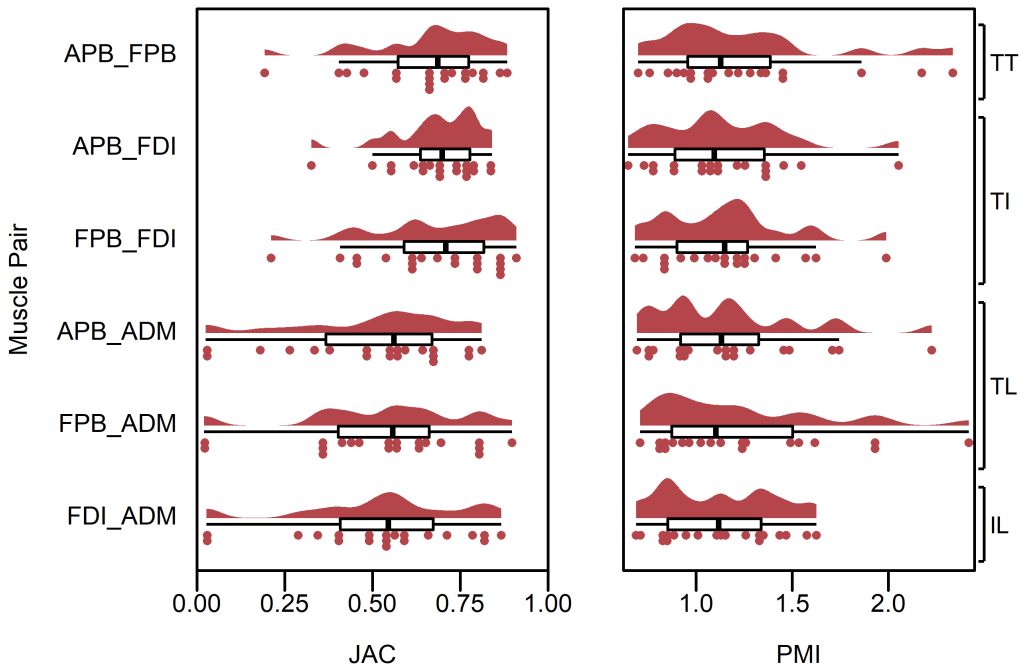

Figure 4: Jaccard index (JAC) and pointwise mutual information (PMI) for hand-hand muscle pairs. Densities were estimated using a Gaussian kernel with standard deviation $\approx$ 0.03, points were binned with a binwidth of 0.02. TT, *Thumb-Thumb*; TI, *Thumb-Index*; TL, *Thumb-Little*; IL, *Index-Little*.

table S2 shows the p-values for subsequent pairwise comparisons. The flexion-flexion muscle pair had a significantly greater Jaccard index than all flexion-extension muscle pairs. A significantly greater Jaccard index was also evident for the extension-extension muscle pair compared to one flexion-extension muscle pair. There also was a significant main effect for pointwise mutual information ($p < 0.001$), and table S3 shows the p-values for subsequent pairwise comparisons. The flexion-flexion muscle pair had significantly greater pointwise mutual information than most flexion-extension muscle pairs. Significantly greater pointwise mutual information was also evident for the extension-extension muscle pair compared to one flexion-extension muscle pair.

Altogether, the Jaccard index but not pointwise mutual information suggests a difference in co-activation dynamics between thumb-index finger and thumb-little finger pairs. In contrast, both outcome measures suggest a difference in co-activation dynamics between wrist flexion-flexion and wrist flexion-extension muscle pairs. According to our simulation, this discrepancy may arise because co-activation dynamics differ for different reasons. Namely, the difference between thumb-index and thumb-little finger muscle pairs may be due to

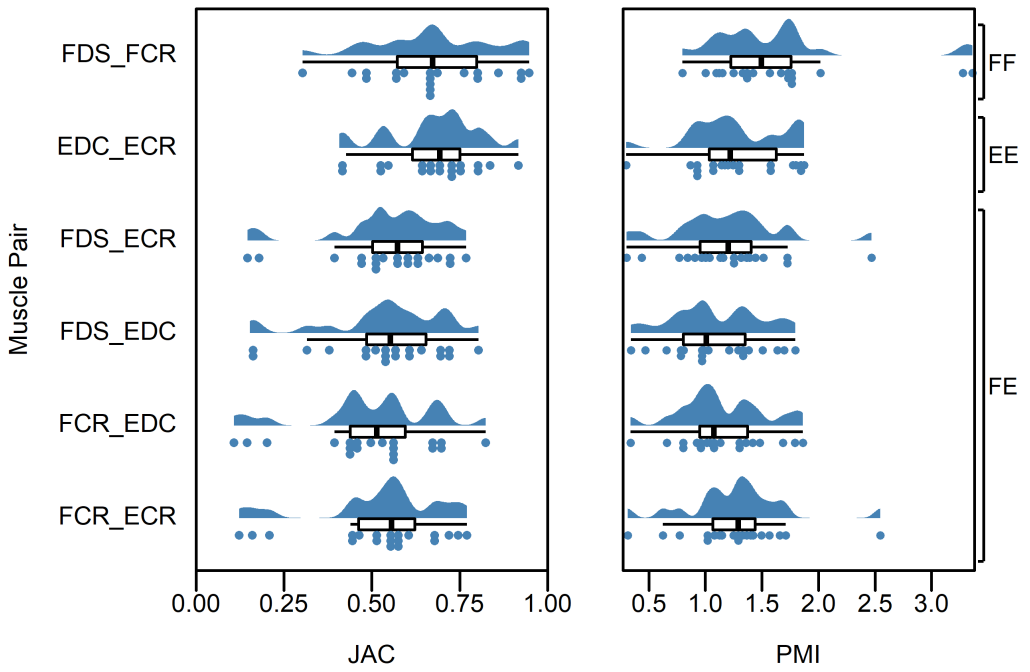

Figure 5: Jaccard index (JAC) and pointwise mutual information (PMI) for forearm-forearm muscle pairs. Densities were estimated using a Gaussian kernel with standard deviation $\approx$ 0.03, points were binned with a binwidth of 0.02. FF, *Flexion-Flexion*; EE, *Extension-Extension*; FE, *Flexion-Extension*.

higher individual response probabilities. Indeed, Figure 6 shows that the index finger muscle (i.e. FDI) tended to have higher response frequencies than the little finger muscle (i.e. AMD). In contrast, the difference between wrist flexion-flexion and wrist flexion-extension pairs may be due to synergistic coupling.

4 Discussion

Using data from pseudorandom TMS over the human cortex, we investigated the co-activation dynamics between different pairs of muscles. Previous studies have used the Jaccard index to quantify co-activation dynamics. We argued that the Jaccard index is not suitable for this purpose and that pointwise mutual information is a better alternative. With that in mind, we employed both measures to our dataset for comparability with previous research and to highlight differences using real data. As for co-activation dynamics, we hypothesized that muscles which are naturally used together — such as thumb and index finger muscles

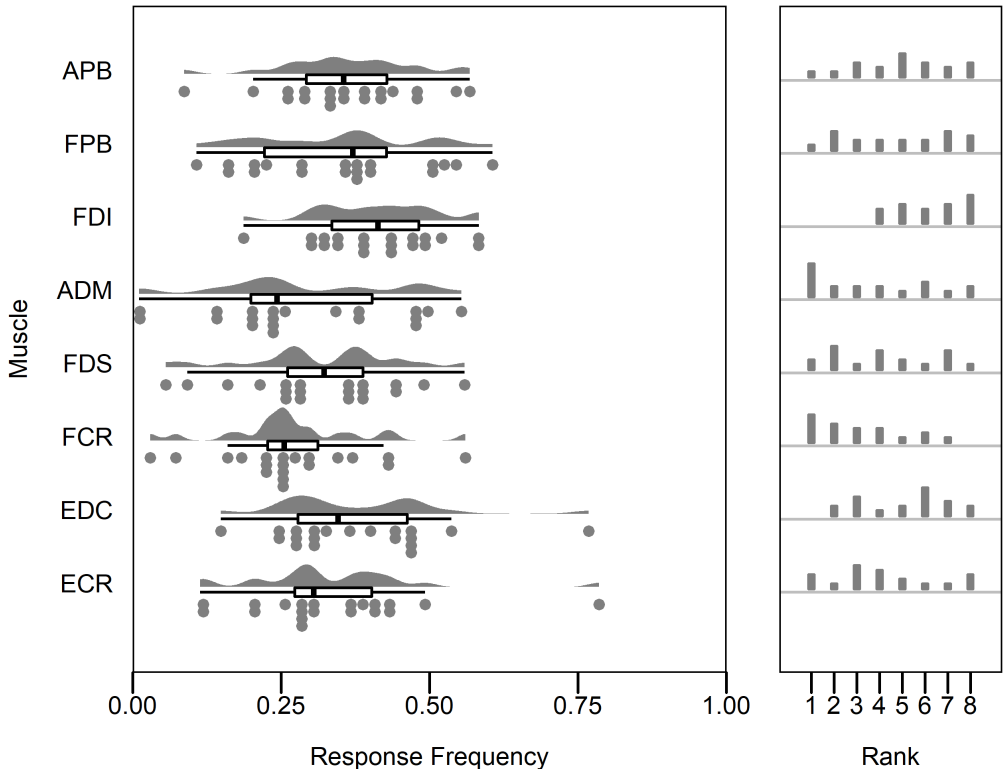

Figure 6: Response frequency and corresponding within-subject rank of all individual muscles. Densities were estimated using a Gaussian kernel with standard deviation ≈ 0.03, points were binned with a binwidth of 0.02.

during precision grip — would be co-activated more often due to synergistic coupling.

We found greater Jaccard indices for thumb-index finger muscle and wrist flexor muscle pairs. However, greater pointwise mutual information was only evident for the wrist flexor muscle pair. Since the Jaccard index, unlike pointwise mutual information, is confounded by the individual probabilities, it is possible that the greater Jaccard index of the thumb-index finger muscle pair is due to greater excitability of the index finger muscle and/or lower excitability of the little finger muscle. Indeed, index finger muscle response frequencies tended to rank high and little finger muscle response frequencies tended to rank low in our dataset. We would like to note that a common finding among previous studies which used the Jaccard index might also be explained by individual excitability. Melgari et al. (2008) and DeJong et al. (2021) reported the greatest Jaccard indices among hand and forearm muscle pairs, and smallest Jaccard indices among muscle pairs involving upper arm muscles. However, hand/forearm muscles are known to be more excitable than upper arm muscles

(Wassermann et al., 1992). Using the Jaccard index, one might be inclined to mistake high excitability for synergistic coupling.

Unlike the thumb-index finger muscle pair, the wrist flexor muscle pair had greater pointwise mutual information than other muscle pairs. This may be due to synergistic coupling. However, alternative explanation cannot be ruled out. For one, this effect may be due to volume conduction / cross-talk (Mesin, 2020), especially given that both wrist flexor muscles (FCR and FDS) are located in close proximity to each other. Yet, we did not find even a weak correlation between MEP amplitude for these muscles (data not shown), which speaks against a cross-talk artefact. Alternatively, the effect could be due insufficient precision of stimulation. That is, at the cortical level, the neural pathways activating each muscle individually may be located in such close proximity that they are less distinguishable given the focality of TMS. We tried to mitigate this issue by choosing a very low stimulation intensity of 105% RMT, thus enhancing the focality of stimulation.

Low spatial selectivity of both cortical stimulation and cortical recording modalities continues to be a major hurdle in the quest to demonstrate synergies in the human nervous system, in general. First, evidence from cortical stimulation suffers from this problem. As the stimulation device generally has to be placed outside the scalp, neuronal targets are farther away. This requires higher stimulation intensities. However, this also means the electric field spreads further tangentially so stimulation is less focal (Deng et al., 2013). Second, evidence from cortical recordings also suffers from this problem. As explained in the introduction, EMG modularity alone does not provide evidence for synergies. However, linking it to EEG would suggest that it is of neural origin, which provides support for synergies. Indeed, cortico-synergy coherence between source-reconstructed EEG recordings from the paracentral lobule and voluntary EMG modules from the lower extremities has been shown during a balance task (Zandvoort et al., 2019). However, these results are compatible with both efferent and afferent information flow between the cortex and EMG modules—as the limited spatial resolution of EEG does hardly allow to distinguish M1 from S1 (and, in addition, coherence is non-directional). Given that both TMS (and other stimulation modalities) and EEG (and MEG) suffer from low spatial selectivity, alternative methods may be needed to demonstrate synergies in humans.

As such, there is a broader question on how to overcome issues of spatial selectivity in demonstrating synergies in the human nervous system. A possible solution is strong field functional magnetic resonance imaging (fMRI). For example, 7T fMRI can provide high

resolution cortical recordings to the point where individual digit representations can be mapped (Arbuckle et al., 2020; Driver et al., 2021; Huber et al., 2020). Unlike its excellent spatial resolution, however, its temporal resolution is low—which is why fMRI cannot be linked with the fast temporal dynamics of EMG. The question remains how to link cortical fMRI recordings to the use of synergies in motor control. One way to answer this is to compare the neural footprint of a "natural" compound movement which likely relies on a synergy to the neural footprint of its individual components. A compound neural footprint that goes beyond a mere combination of individual neural footprints would suggest a synergy. This comparison could be repeated using a "unnatural" compound movement which likely does not rely on a synergy. Here, the compound neural footprint should be a combination of individual neural footprints. The spatial precision of 7T fMRI allows to pinpoint such effects to M1, which would make a strong case that the effects reflect efferent information flow, thus circumventing the limitation when linking EMG modules with EEG. To strengthen this point, the fMRI approach could be supplemented with TMS in the same subjects, as effects from neural stimulation must reflect efferent information flow. TMS could be carried out during active movement (where excitability is higher and thus lower stimulation intensities can be used) following the same principles as the fMRI protocol (i.e. compare compound neural footprints to a combination of their individual components).

To conclude, we used TMS in order to learn about possible synergistic coupling in a set of hand and forearm muscles. We argued that, in this research context, the Jaccard index is inappropriate for quantifying pairwise co-activation dynamics and pointwise mutual information should be used instead. We also demonstrated the discrepancy between these two measures on our data. Our results are compatible with synergistic coupling between wrist flexor muscles. However, this finding needs to be interpreted with caution, in light of the spatial selectivity of TMS.

Acknowledgments

Thank you to Fang Jin for providing the data and for fruitful discussions.

References

Amundsen Huffmaster, S. L., Van Acker, G. M., Luchies, C. W., & Cheney, P. D. (2017). Muscle synergies obtained from comprehensive mapping of the primary motor cortex forelimb representation using high-frequency, long-duration ICMS. *Journal of Neurophysiology*, *118*(1), 455–470. https://doi.org/10.1152/jn.00784.2016

Arbuckle, S. A., Weiler, J., Kirk, E. A., Rice, C. L., Schieber, M., Pruszynski, J. A., Ejaz, N., & Diedrichsen, J. (2020). Structure of population activity in primary motor cortex for single finger flexion and extension [Publisher: Society for Neuroscience Section: Research Articles]. *Journal of Neuroscience*, *40*(48), 9210–9223. https://doi.org/10.1523/JNEUROSCI.0999-20.2020

Bach, M. M., Daffertshofer, A., & Dominici, N. (2021). Muscle synergies in children walking and running on a treadmill. *Frontiers in Human Neuroscience*, *15*. https://doi.org/10.3389/fnhum.2021.637157

Bernstein, N. (1966). *The co-ordination and regulation of movements*. Pergamon Press. Retrieved May 25, 2021, from https://ci.nii.ac.jp/naid/10008376164/

Cheung, V. C. K., & Seki, K. (2021). Approaches to revealing the neural basis of muscle synergies: A review and a critique [Publisher: American Physiological Society]. *Journal of Neurophysiology*, *125*(5), 1580–1597. https://doi.org/10.1152/jn.00625.2019

Chung, N. C., Miasojedow, B., Startek, M., & Gambin, A. (2019). Jaccard/tanimoto similarity test and estimation methods for biological presence-absence data. *BMC Bioinformatics*, *20*(15), 644. https://doi.org/10.1186/s12859-019-3118-5

d'Avella, A., Portone, A., Fernandez, L., & Lacquaniti, F. (2006). Control of fast-reaching movements by muscle synergy combinations. *The Journal of Neuroscience*, *26*(30), 7791–7810. https://doi.org/10.1523/JNEUROSCI.0830-06.2006

DeJong, S. L., Bisson, J. A., Darling, W. G., & Shields, R. K. (2021). Simultaneous recording of motor evoked potentials in hand, wrist and arm muscles to assess corticospinal divergence. *Brain Topography*, *34*(4), 415–429. https://doi.org/10.1007/s10548-021-00845-1

Deng, Z.-D., Lisanby, S. H., & Peterchev, A. V. (2013). Electric field depth–focality tradeoff in transcranial magnetic stimulation: Simulation comparison of 50 coil designs. *Brain stimulation*, *6*(1), 1–13. https://doi.org/10.1016/j.brs.2012.02.005

Desmurget, M., Richard, N., Harquel, S., Baraduc, P., Szathmari, A., Mottolese, C., & Sirigu, A. (2014). Neural representations of ethologically relevant hand/mouth synergies in the human precentral gyrus. *Proceedings of the National Academy of Sciences of*

the United States of America, *111*(15), 5718–5722. https://doi.org/10.1073/pnas.1321909111

Dominici, N., Ivanenko, Y. P., Cappellini, G., d'Avella, A., Mondì, V., Cicchese, M., Fabiano, A., Silei, T., Paolo, A. D., Giannini, C., Poppele, R. E., & Lacquaniti, F. (2011). Locomotor primitives in newborn babies and their development [Publisher: American Association for the Advancement of Science Section: Report]. *Science*, *334*(6058), 997–999. https://doi.org/10.1126/science.1210617

Driver, I. D., Panchuelo, R. M. S., Mougin, O., Asghar, M., Kolasinski, J., Clarke, W. T., Rua, C., Morgan, A. T., Carpenter, A., Muir, K., Porter, D., Rodgers, C. T., Clare, S., Wise, R. G., Bowtell, R., & Francis, S. T. (2021, April 1). *Multi-centre, multi-vendor 7 tesla fMRI reproducibility of hand digit representation in the human somatosensory cortex* [Company: Cold Spring Harbor Laboratory Distributor: Cold Spring Harbor Laboratory Label: Cold Spring Harbor Laboratory Section: New Results Type: article]. https://doi.org/10.1101/2021.03.25.437006

Gentner, R., & Classen, J. (2006). Modular organization of finger movements by the human central nervous system. *Neuron*, *52*(4), 731–742. https://doi.org/10.1016/j.neuron.2006.09.038

Graziano, M. S. A. (2016). Ethological action maps: A paradigm shift for the motor cortex. *Trends in Cognitive Sciences*, *20*(2), 121–132. https://doi.org/10.1016/j.tics.2015.10.008

Huber, L., Finn, E. S., Handwerker, D. A., Bönstrup, M., Glen, D. R., Kashyap, S., Ivanov, D., Petridou, N., Marrett, S., Goense, J., Poser, B. A., & Bandettini, P. A. (2020). Sub-millimeter fMRI reveals multiple topographical digit representations that form action maps in human motor cortex. *NeuroImage*, *208*, 116463. https://doi.org/10.1016/j.neuroimage.2019.116463

Ingram, J. N., Körding, K. P., Howard, I. S., & Wolpert, D. M. (2008). The statistics of natural hand movements. *Experimental brain research. Experimentelle Hirnforschung. Experimentation cerebrale*, *188*(2), 223–236. https://doi.org/10.1007/s00221-008-1355-3

Ivanenko, Y. P., Poppele, R. E., & Lacquaniti, F. (2004). Five basic muscle activation patterns account for muscle activity during human locomotion. *The Journal of Physiology*, *556*(1), 267–282. https://doi.org/https://doi.org/10.1113/jphysiol.2003.057174

Jaccard, P. (1912). The distribution of the flora in the alpine zone. *New Phytologist*, *11*(2), 37–50. https://doi.org/10.1111/j.1469-8137.1912.tb05611.x

Jin, F., Bruijn, S., & Daffertshofer, A. (2021, July 30). *A new protocol for multiple muscle mapping using nTMS* [Section: New Results Type: article]. bioRxiv. https://doi.org/10.1101/2021.07.29.454279

Kassambara, A. (2021, February 13). *Rstatix: Pipe-friendly framework for basic statistical tests* (Version 0.7.0). Retrieved March 12, 2022, from https://CRAN.R-project.org/package=rstatix

Kutch, J. J., & Valero-Cuevas, F. J. (2012). Challenges and new approaches to proving the existence of muscle synergies of neural origin [Publisher: Public Library of Science]. *PLOS Computational Biology*, *8*(5), e1002434. https://doi.org/10.1371/journal.pcbi.1002434

Maier, M. A., & Hepp-Reymond, M.-C. (1995). EMG activation patterns during force production in precision grip. *Experimental Brain Research*, *103*(1), 108–122. https://doi.org/10.1007/BF00241969

Mangiafico, S. (2022, January 3). *Rcompanion: Functions to support extension education program evaluation* (Version 2.4.13). Retrieved March 12, 2022, from https://CRAN.R-project.org/package=rcompanion

Melgari, J.-M., Pasqualetti, P., Pauri, F., & Rossini, P. M. (2008). Muscles in "concert": Study of primary motor cortex upper limb functional topography. *PloS One*, *3*(8), e3069. https://doi.org/10.1371/journal.pone.0003069

Mesin, L. (2020). Crosstalk in surface electromyogram: Literature review and some insights. *Physical and Engineering Sciences in Medicine*, *43*(2), 481–492. https://doi.org/10.1007/s13246-020-00868-1

Müller, K., & Bryan, J. (2020, December 13). *Here: A simpler way to find your files* (Version 1.0.1). Retrieved March 12, 2022, from https://CRAN.R-project.org/package=here

Nollet, H., Van Ham, L., Deprez, P., & Vanderstraeten, G. (2003). Transcranial magnetic stimulation: Review of the technique, basic principles and applications. *The Veterinary Journal*, *166*(1), 28–42. https://doi.org/10.1016/S1090-0233(03)00025-X

Oliveira, A. S., Gizzi, L., Ketabi, S., Farina, D., & Kersting, U. G. (2016). Modular control of treadmill vs overground running. *PLoS ONE*, *11*(4). https://doi.org/10.1371/journal.pone.0153307

Overduin, D'Avella, A., Carmena, J. M., & Bizzi, E. (2014). Muscle synergies evoked by microstimulation are preferentially encoded during behavior [Publisher: Frontiers]. *Frontiers in Computational Neuroscience*, *8*. https://doi.org/10.3389/fncom.2014.00020

Overduin, d'Avella, A., Carmena, J. M., & Bizzi, E. (2012). Microstimulation activates a handful of muscle synergies. *Neuron*, *76*(6), 1071–1077. https://doi.org/10.1016/j.neuron.2012.10.018

Overduin, d'Avella, A., Roh, J., & Bizzi, E. (2008). Modulation of muscle synergy recruitment in primate grasping. *The Journal of Neuroscience*, *28*(4), 880–892. https://doi.org/10.1523/JNEUROSCI.2869-07.2008

Pedersen, T. L. (2020, December 17). *Patchwork: The composer of plots* (Version 1.1.1). Retrieved March 12, 2022, from https://CRAN.R-project.org/package=patchwork

Pohlert, T. (2021, November 13). *PMCMRplus: Calculate pairwise multiple comparisons of mean rank sums extended* (Version 1.9.3). Retrieved March 12, 2022, from https://CRAN.R-project.org/package=PMCMRplus

R Core Team, .-. (2021, November 1). *R: A language and environment for statistical computing* (Version 4.1.2). Vienna, Austria, R Foundation for Statistical Computing. https://www.R-project.org/

Salvatore, S., Dagestad Rand, K., Grytten, I., Ferkingstad, E., Domanska, D., Holden, L., Gheorghe, M., Mathelier, A., Glad, I., & Kjetil Sandve, G. (2020). Beware the jaccard: The choice of similarity measure is important and non-trivial in genomic colocalisation analysis. *Briefings in Bioinformatics*, *21*(5), 1523–1530. https://doi.org/10.1093/bib/bbz083

Sanchez, G. (2013, December 19). *Colortools: Tools for colors in a hue-saturation-value (HSV) color model* (Version 0.1.5). Retrieved March 12, 2022, from https://CRAN.R-project.org/package=colortools

Santuz, A., Brüll, L., Ekizos, A., Schroll, A., Eckardt, N., Kibele, A., Schwenk, M., & Arampatzis, A. (2020). Neuromotor dynamics of human locomotion in challenging settings. *iScience*, *23*(1), 100796. https://doi.org/10.1016/j.isci.2019.100796

Sherrington, C. (1952). *The integrative action of the nervous system* [Google-Books-ID: CRU8AAAAIAAJ]. CUP Archive.

Shinoda, Y., Yokota, J., & Futami, T. (1981). Divergent projection of individual corticospinal axons to motoneurons of multiple muscles in the monkey. *Neuroscience Letters*, *23*(1), 7–12. https://doi.org/10.1016/0304-3940(81)90182-8

Steele, K. M., Tresch, M. C., & Perreault, E. J. (2015). Consequences of biomechanically constrained tasks in the design and interpretation of synergy analyses. *Journal of Neurophysiology*, *113*(7), 2102–2113. https://doi.org/10.1152/jn.00769.2013

Takei, T., Confais, J., Tomatsu, S., Oya, T., & Seki, K. (2017). Neural basis for hand muscle synergies in the primate spinal cord. *Proceedings of the National Academy*

of Sciences of the United States of America, *114*(32), 8643–8648. https://doi.org/10.1073/pnas.1704328114

Takei, T., & Seki, K. (2010). Spinal interneurons facilitate coactivation of hand muscles during a precision grip task in monkeys. *The Journal of Neuroscience*, *30*(50), 17041–17050. https://doi.org/10.1523/JNEUROSCI.4297-10.2010

Warnes, G. R., Bolker, B., Gorjanc, G., Grothendieck, G., Korosec, A., Lumley, T., MacQueen, D., Magnusson, A., Rogers, J., & others and, a. (2017, June 6). *Gdata: Various r programming tools for data manipulation* (Version 2.18.0). Retrieved March 12, 2022, from https://CRAN.R-project.org/package=gdata

Wassermann, E. M., McShane, L. M., Hallett, M., & Cohen, L. G. (1992). Noninvasive mapping of muscle representations in human motor cortex. *Electroencephalography and Clinical Neurophysiology/Evoked Potentials Section*, *85*(1), 1–8. https://doi.org/10.1016/0168-5597(92)90094-R

Wickham, H., & RStudio. (2021, April 15). *Tidyverse: Easily install and load the 'tidyverse'* (Version 1.3.1). Retrieved March 12, 2022, from https://CRAN.R-project.org/package=tidyverse

Zandvoort, C. S., van Dieën, J. H., Dominici, N., & Daffertshofer, A. (2019). The human sensorimotor cortex fosters muscle synergies through cortico-synergy coherence. *NeuroImage*, *199*, 30–37. https://doi.org/10.1016/j.neuroimage.2019.05.041

Supplementary Material

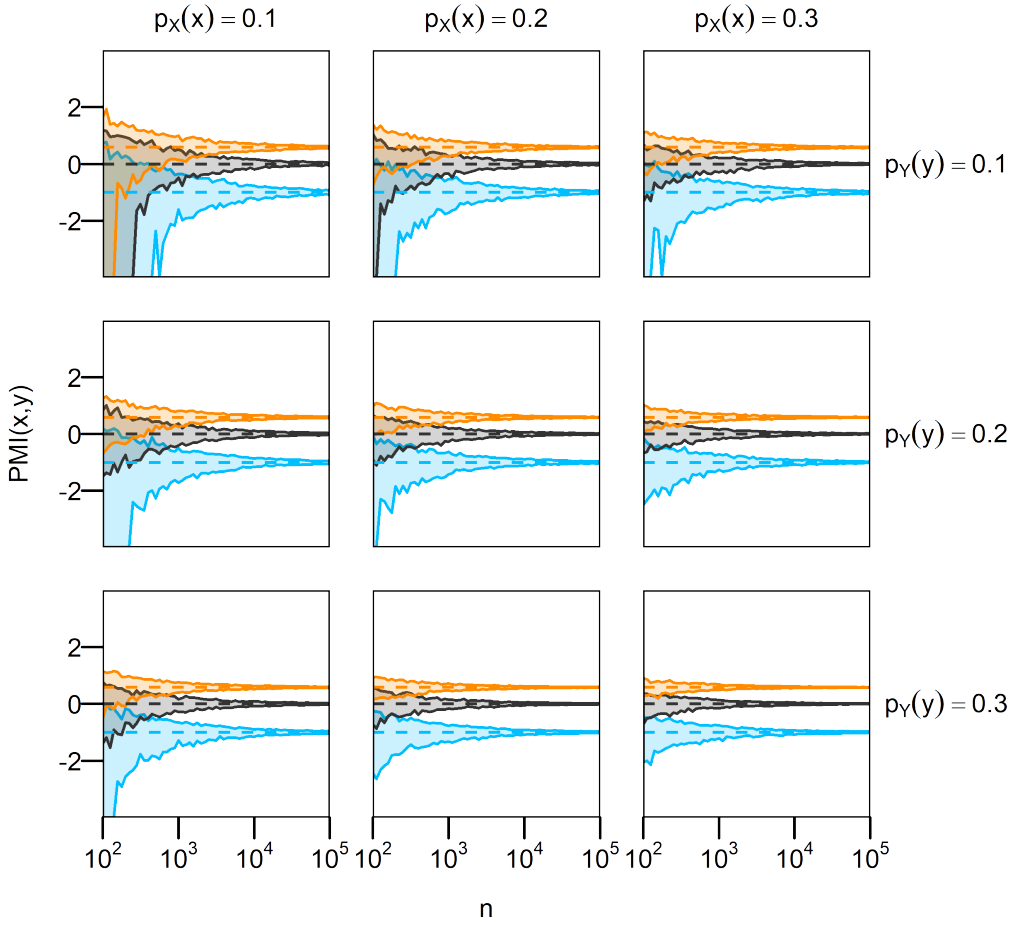

Figure S1: 10th to 90th percentile of estimated pointwise mutual information across 100 repetitions. The ground truth is $\mathrm{R}(x, y) = 0.5, 1, 1.5 \Rightarrow \mathrm{PMI}(x, y) = -1, 0, \sim 0.6$, marked by the dashed lines. *Note:* This figure highlights how the spread of pointwise mutual information estimates depends on n, for given individual probabilities. When n is too low to reliably estimate the individual and joint probabilities, pointwise mutual information estimates vary strongly and thus overlap considerably.

		Thumb-Thumb	Thumb-Index		Thumb-Little		Index-Little
		APB-FPB	APB-FDI	FPB-FDI	FPB-ADM	APB-ADM	FDI-ADM
Thumb-Thumb	APB-FPB	-	1.000	0.974	**0.017**	0.114	0.074
Thumb-Index	APB-FDI	1.000	-	0.985	**0.013**	0.092	0.059
	FPB-FDI	0.974	0.985	-	**0.001**	**0.013**	**0.007**
Thumb-Little	APB-ADM	**0.017**	**0.013**	**0.001**	-	0.985	0.996
	FPB-ADM	0.114	0.092	**0.013**	0.985	-	1.000
Index-Little	FDI-ADM	0.074	0.059	**0.007**	0.996	1.000	-

Table S1: P-values for pairwise comparisons of the Jaccard index between hand muscle pairs, with $p < 0.05$ highlighted in bold.

		Flexion-Flexion	Extension-Extension	Flexion-Extension			
		FDS-FCR	EDC-ECR	FDS-ECR	FDS-EDC	FCR-EDC	FCR-ECR
Flexion-Flexion	FDS-FCR	-	0.959	**0.009**	**0.013**	$<$ **.001**	**0.005**
Extension-Extension	EDC-ECR	0.959	-	0.114	0.139	$<$ **.001**	0.074
Flexion-Extension	FDS-ECR	**0.009**	0.114	-	1.000	0.482	1.000
	FDS-EDC	**0.013**	0.139	1.000	-	0.428	1.000
	FCR-EDC	$<$ **.001**	$<$ **.001**	0.482	0.428	-	0.595
	FCR-ECR	**0.005**	0.074	1.000	1.000	0.595	-

Table S2: P-values for pairwise comparisons of the Jaccard index between forearm muscle pairs, with $p < 0.05$ highlighted in bold.

		Flexion-Flexion	Extension-Extension	Flexion-Extension			
		FDS-FCR	EDC-ECR	FDS-ECR	FDS-EDC	FCR-EDC	FCR-ECR
Flexion-Flexion	FDS-FCR	-	0.092	$<$ **.001**	$<$ **.001**	$<$ **.001**	0.059
Extension-Extension	EDC-ECR	0.092	-	0.482	**0.047**	0.428	1.000
Flexion-Extension	FDS-ECR	$<$ **.001**	0.482	-	0.882	1.000	0.595
	FDS-EDC	$<$ **.001**	**0.047**	0.882	-	0.913	0.074
	FCR-EDC	$<$ **.001**	0.428	1.000	0.913	-	0.538
	FCR-ECR	0.059	1.000	0.595	0.074	0.538	-

Table S3: P-values for pairwise comparisons of the pointwise mutual information between forearm muscle pairs, with $p < 0.05$ highlighted in bold.